

# Simulation of fatigue failure in a full composite wind turbine blade

Mahmood M. Shokrieh<sup>\*</sup>, Roham Rafiee

*Composites Research Laboratory, Mechanical Engineering Department, Iran University of Science and Technology, Narmak, Tehran 16844, Iran*

Available online 13 June 2005

## Abstract

Lifetime prediction of a horizontal axis wind turbine composite blade is considered. Load cases are identified, calculated and evaluated. Static analysis is performed with a full 3-D finite element method and the critical zone where fatigue failure begins is extracted. Accumulated fatigue damage modeling is employed as a damage estimation rule based on generalized material property degradation. Since wind flow (loading) is random, a stochastic approach is employed to develop a computer code in order to simulate wind flow with randomness in its nature on the blade and subsequently each load case is weighted by its rate of occurrence using a Weibull wind speed distribution.

© 2005 Elsevier Ltd. All rights reserved.

*Keywords:* Composites; Finite element; Stochastic; Wind turbine blade; Damage; Failure analysis

## 1. Introduction

Pollution free electricity generation, fast installation and commissioning capability, low operation and maintenance cost and taking advantage of using free and renewable energies are all advantages of using wind turbines as an electricity generators. Along with these advantages, the main disadvantage of this industry is the temporary nature of wind flow. Therefore, using reliable and efficient equipment is necessary in order to get as much as energy from wind during the limited period of time that it flows strongly.

The blade is the most important component in a wind turbine which nowadays is designed according to a refined aerodynamic science in order to capture the maximum energy from the wind flow. Blades of horizontal axis are now completely made of composite materials. Composite materials satisfy complex design constraints such as lower weight and proper stiffness, while providing good resistance to the static and fatigue loading.

Generally, wind turbines are fatigue critical machines and the design of many of their components (especially blades) are dictated by fatigue considerations. Several factors expose wind turbine blades to the fatigue phenomena which can be summarized as shown below [1]:

1. Long and flexible structures
2. Vibrations in its resonant mode
3. Randomness in the load spectra due to the nature of the wind
4. Continuous operation under different conditions
5. Low maintenance during lifetime

A wind turbine blade expects to sustain its mission for about 20–30 years. Fig. 1 shows a comparison between different industrial components and their expected life cycles.

The above mentioned reasons and extensive expected lifetime cause design constraints for wind turbine structures that fall into either extreme load or fatigue categories. For the case of extreme load design, the load estimation problem is limited to finding a single maximum load level that the structure can tolerate. For design against fatigue, however, loads must be defined

<sup>\*</sup> Corresponding author. Tel./fax: +98 21 749 1206.  
E-mail address: [shokrieh@iust.ac.ir](mailto:shokrieh@iust.ac.ir) (M.M. Shokrieh).

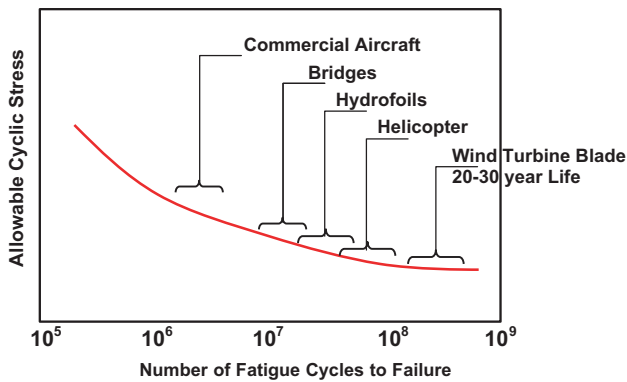


Fig. 1. Schematic  $S$ – $N$  curves for different industrial components [1].

for all input conditions and then summed over the distribution of input conditions weighted by the relative frequency of occurrence.

Most ongoing research on fatigue phenomena uses load spectra obtained by digital sampling of a specific configuration of strain gauges which read the strain at a specific location near the root of blade. Then, the representative sample of each load spectrum is weighted by its rate of occurrence that can be obtained from the statistical study of the wind pattern. Finally all weighted load spectra are summed and total load spectrum is derived. This load spectrum is utilized to estimate fatigue damage in the blade using Miner's rule [2]. One of the main shortcomings of this method is the linear nature of Miner's rule. Not only is Miner's rule not a proper rule for fatigue consideration in metals, but also it has been proven that this rule is not suitable for composites [3]. Another problem with using Miner's rule is the weakness of this model to simulate the load sequence and history of load events. This shortcoming can clearly be seen in the difference of predicted lifetimes of blades with two orders of magnitudes for two load cases with different load sequences [2]. Furthermore, most investigations in fatigue simulation of composite blades are limited to the deterministic approach. In addition, identification of a place to install the strain gauges in order to extract the load spectrum is also questionable. Using a massive and high cost material fatigue database [4], is another problem with these methods. It forces researchers to characterize each configuration of lay-up separately and is the main reason for publishing new versions of these databases each year due to introduction of new lay-up configurations in blade structure by industry.

## 2. State of the art

In this paper, a model to study the fatigue phenomena for wind turbine composite blades is presented in order to overcome the aforementioned shortcomings

of current methods. As a case study, a 23 m blade of a V47-660 wind turbine, manufactured by the Vestas Company, was selected. Firstly, loading on the blade is considered carefully using the finite element method and the critical zone where catastrophic fatigue failure initiates is determined. Then, each load case is weighted and finally fatigue is studied using a developed stiffness degradation method. The main advantages of this method can be expressed in its ability to simulate the load sequence and load history. Due to randomness of wind flow; stochastic analysis will be employed instead of deterministic analysis. Based on the capability of the method for fatigue modeling, performing a large quantity of experiments in order to characterize complete fatigue behavior of materials is avoided.

## 3. Modeling

The investigated blade consists of three main parts called shell, spar and root-joint (see Fig. 2).

The shell is responsible to help create the required pressure distribution on the blade. The cross sections of the blade are different airfoils based on aerodynamic considerations. The shell also twists about  $15^\circ$  due to aerodynamic reasons and also has a tapered shape from root to tip.

A brief summary of pertinent data related to the investigated blade is shown in Table 1.

The spar, which is also called the main beam, has to support loads on the blade that arise from different sources. The shell structure carries only 20% of total loads while the rest has to be carried by the spar. The cross section of the spar has a box shape.

The root joint is the only metallic part in the current blade that connects whole blade structure to the hub by screws. This metallic joint is covered by composite laminates internally and externally.

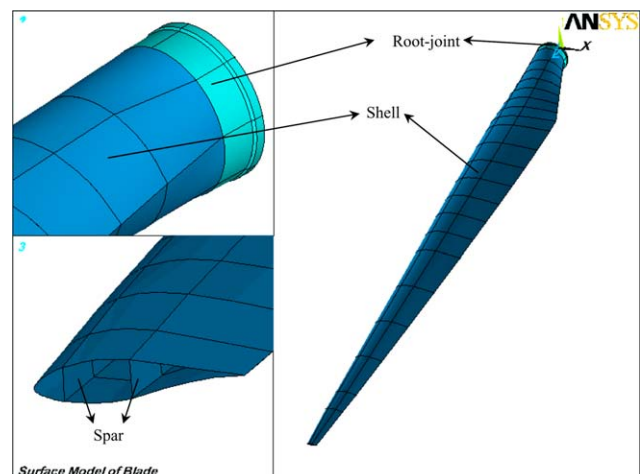


Fig. 2. Depiction of root-joint, shell and spar.

Table 1  
General specifications of investigated blade

Length	22,900 mm
Maximum chord	2087 mm
Station of maximum chord	R4500
Minimum chord	282.5 mm
Twist	15.17°
Station of CG	R8100
Weight of blade	1250 kg
Tip to tower distance	4.5 m
Surface area	28 m <sup>2</sup>
Airfoil cross-section types	FFA-W3, NACA-63-xxx, MIX

In order to provide data for the finite element model, a geometrical model was created based on cross section profiles of shell and spar using Auto-CAD [5] software. Then the wire frame model, which is the fundamental geometrical model, was transferred to ANSYS finite element software [6]. After that, geometrical modeling was completed by creating surfaces using the loft method. In the meshing process, second order shell elements were employed to increase accuracy of the modeling. In addition, the selected element type is compatible with composites and, in order to not having any triangular elements, a manual meshing method was employed. Therefore all elements have quadratic shape with 8 nodes and acceptable aspect ratio. Elements of the root-joint segment are second order cubic solid elements.

Convergence criteria should be considered to evaluate the results. Convergence analysis is performed on a metallic model of the blade. By improving mesh density step-by-step a suitable number of elements is obtained. The stabilization of tip deflection and Von-Misses equivalent stress at a location far from the applied loads are the criteria of convergence. Also in order to examine the case with both bending and torsion in the structure, the loads were applied on the trailing edge and bound-

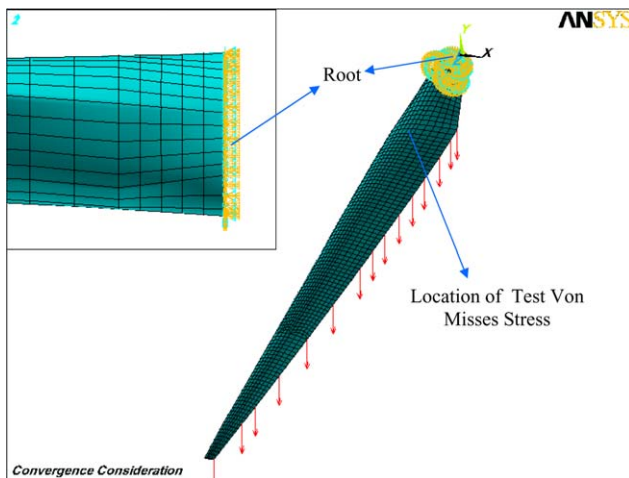


Fig. 3. Finite element model of turbine blade showing loads and boundary conditions for convergence consideration.

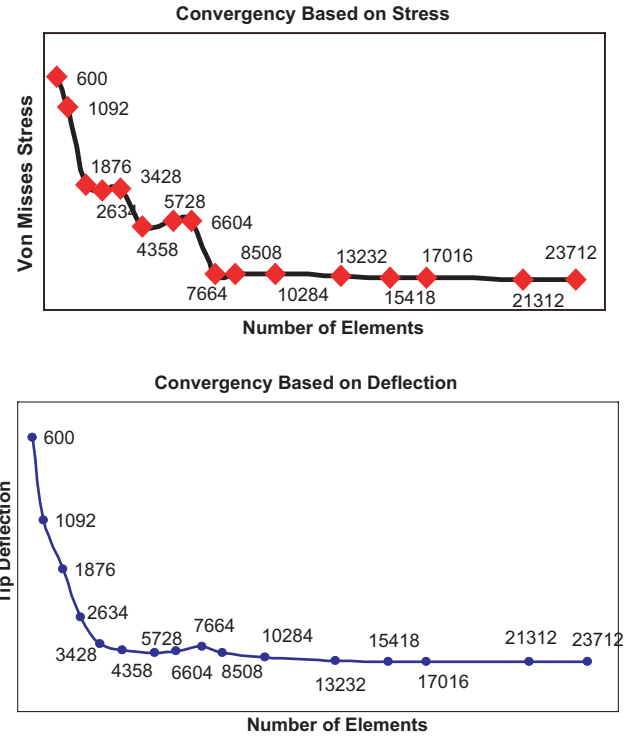


Fig. 4. Convergence graphs of FE model.

ary conditions consisted of fixing all 6 degrees of freedom of nodes that are placed at the root. The depiction of the FE model is shown in Fig. 3.

Fig. 4 shows the results of convergence analysis. From Fig. 4, it is clear that convergence is obtained with the use of about 10,000 or more elements.

#### 4. Material characterization

The investigated blade consists of three main types of pre-preg glass/epoxy composites: Unidirectional plies, bi-axial and tri-axial materials.

Bi-axial and tri-axial plies contain two and three same unidirectional fabrics, respectively, which are stitched together (thus are not woven). The main reason for not using woven form of composites is due to disadvantages of using them based on their fatigue properties. In the woven form, due to out-of-plane curvature of fabrics, stress concentrations happen and consequently fatigue performance of these materials decreases dramatically [3].

Tri-axial and bi-axial fabrics are used in the shell structure and unidirectional and bi-axial are used in the spar structure. The configuration of the bi-axial lamina is [0/90]<sub>T</sub> and the configuration of the tri-axial laminate is [0/+45/-45]<sub>T</sub>. Two kinds of foam (PMI and PVC) are used respectively at the spar and shell locations, respectively, in order to construct the sandwich panel.

The required properties for analyzing the structure are mechanical and strength properties where the first group is used for stress analysis and the second one is used for failure analysis [7]. Material characterization is used to extract the aforementioned properties. Full material properties of the U-D fabric are available experimentally [4] but for the bi-axial and tri-axial composites, the mechanical properties are not complete. The available data of these materials are limited to the elastic modulus in the 0° and 45° directions [8]. The bi-axial and tri-axial laminates and the direction where the experimental results are available are shown in Fig. 5. The available experimental data are summarized in Table 2.

As it can be seen from Table 2, elastic modulus  $E_1$  and  $E_2$  are equal in both [+45/−45]<sub>T</sub> and [0/90]<sub>T</sub> and [0/90/−45]<sub>T</sub> due to symmetry.

4.1. Extracting non-available mechanical properties

First, stiffness matrices of tri-axial and bi-axial materials are calculated by considering the proportion of fabric in each direction and then the matrices were inverted. In parallel, compliance matrices based on available data were made and finally the recently obtained compliance matrices were compared to the previously extracted compliance matrices from the stiffness matrices. Finally, after omitting redundant equations, the remaining ones form 14 sets of equations with 14 unknowns enabling the solution for the mechanical properties of constructed unidirectional plies.

Those equations are not reported here due to space limitations and complete list of the governing equations

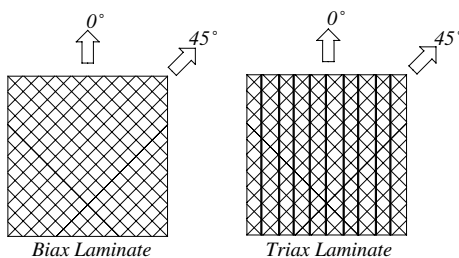


Fig. 5. Experiment directions of bi-axial and tri-axial laminates.

Table 2 Available and non-available mechanical properties [4,8]

Composites	Configuration	$E_1$ [GPa]	$E_2$ [GPa]	$\nu_{12}$	$E_6$ [GPa]
Unidirectional	–	43	9.77	0.32	3.31
Bi-axial	[±45] <sub>T</sub>	6.8	6.8	N/A <sup>a</sup>	N/A
Bi-axial	[0/90] <sub>T</sub>	16.7	16.7	N/A	N/A
Tri-axial	[0/±45] <sub>T</sub>	20.7 ± 3.1	N/A	N/A	N/A
Tri-axial	[0/90/−45] <sub>T</sub>	15.1 ± 2.3	15.1 ± 2.3	N/A	N/A

<sup>a</sup> N/A: Not available.

can be found in Ref. [9]. Due to this fact that those 14 equations are highly dependent and nonlinear, solving them by conventional method is impossible and it needs a start point. The best suggestion for a starting point is the Poisson’s ratio for the bi-axial material in configuration of [0/90]<sub>T</sub>. Experiments show that the Poisson’s ratio of [0/90]<sub>T</sub> configuration is somewhere between 0.05 and 0.1 and these values also are verified by theory [10]. In Table 3, the results obtained by using different amount of Poisson’s ratio are summarized.

As can be seen, the best results are achieved when Poisson’s ratio is set to 0.06 because of its  $E_Y$ . Therefore, mechanical properties of unidirectional plies are available from experiments [4] and mechanical properties of bi-axial and tri-axial laminates can be calculated based on the technique in this research and using mechanical properties of their constructed U-D ply which is calculated and inserted in Table 3. The mechanical properties are summarized in Table 4.

If we calculate the flexural modulus using the obtained data, there is very good agreement to the experimentally available value for this parameter as shown in Table 5.

One of the main advantages of using the inverse method can be realized in the fatigue modeling method that is employed in this paper and will be discussed later in detail.

Table 3 Mechanical properties of constructed U-D ply varied by change in major Poisson’s ratio of bi-axial laminate

MPB <sup>a</sup>	$E_X$ [GPa]	$E_Y$ [GPa]	$\nu$	$G$ [GPa]
0.05	28.549	4.5643	.21	2.107
0.06	28.892	4.3624	.26	2.096
0.07	29.010	4.2215	.32	2.090
0.08	29.127	4.100	.37	2.085
0.09	29.197	3.8240	.40	2.080
0.10	29.234	3.6942	.43	2.077

<sup>a</sup> MPB: Major Poisson’s ratio of bi-axial [0/90]<sub>T</sub>.

Table 4 Mechanical properties of involved materials in the blade

	$E_1$ [GPa]	$E_2$ [GPa]	Major Poisson’s ratio	$G_{XY}$ [GPa]
Unidirectional ply	43	9.77	0.32	3.31
Bi-axial [0/90] <sub>T</sub>	16.7	16.7	0.06	2.01
Tri-axial [0/+45/−45] <sub>T</sub>	17.6	7.01	0.52	5.07

Table 5 Experimental and theoretical comparison of flexural modulus

	Tri-axial [0/90/−45]		Tri-axial [0/45/−45]	
Flexural modulus	Experimental [8]	Theoretical	Experimental [8]	Theoretical
	15.1 ± 2.3	15.23	16.7 ± 2.5	17.85

Table 6  
Mass comparison of the blade

	Mass [kg]	CG location [mm]
FE model	1268.45	7575.23 (from the root)
Realistic	1250.00	7500.00 (from the root)

The last step of this stage is devoted to extracting the weight of the finite element model and comparing it with realistic data. These data are shown in Table 6 and describe the health of model from lay-up configuration and prove that the model is in a good accordance with actual structures.

## 5. Loading

The load cases are determined by the combination of specific operating and external conditions. Operating and external conditions are assumed to be statistically independent [11]. Operating conditions divided into four groups known as normal, fault, after occurrence of the fault and transportation, erection and maintenance (see Fig. 6). External conditions are divided into two groups called normal and extreme. The load cases to be used for fatigue analysis generally arise only from the combination of normal external and operating conditions. It is assumed in this context that because they occur so rarely, the other combinations will not have any significant effect on fatigue strength [11].

The involved subgroups of normal operating and normal external conditions are shown in Fig. 6.

All of the load cases that occur during the mentioned events can be categorized as follows:

1. Aerodynamic loads on the blade
2. Weight of the blade
3. Annual gust
4. Changes in the wind direction
5. Centrifugal force
6. Force that arise from start/stop angular acceleration
7. Gyroscopic forces due to yaw movements
8. Activation of mechanical brake
9. Thermal effect

All of the above load cases were calculated and it was evident that gyroscopic forces and forces from mechanical brake activation can be ignored in comparison with the other loads [12]. A temperature range was considered between  $-10^{\circ}$  and  $+40^{\circ}$  according to the surrounding ambient environment.

## 6. Static analysis

At the first step of static analysis, in order to insure that the model is compatible with real structures, a free vibration analysis of model is performed [12]. The resulting data are in a good agreement with experimental data [12]. The results of free vibration analysis show that model is in accordance with real structures from different aspects such as dimension, material properties and lay-up sequence.

In the second step, calculated forces from the previous section are applied and the response of the structure is studied. In some cases, performing non-linear analysis was necessary due to large rotation effects as a source of non-linearity. The results of these analyses are summarized in Table 7.

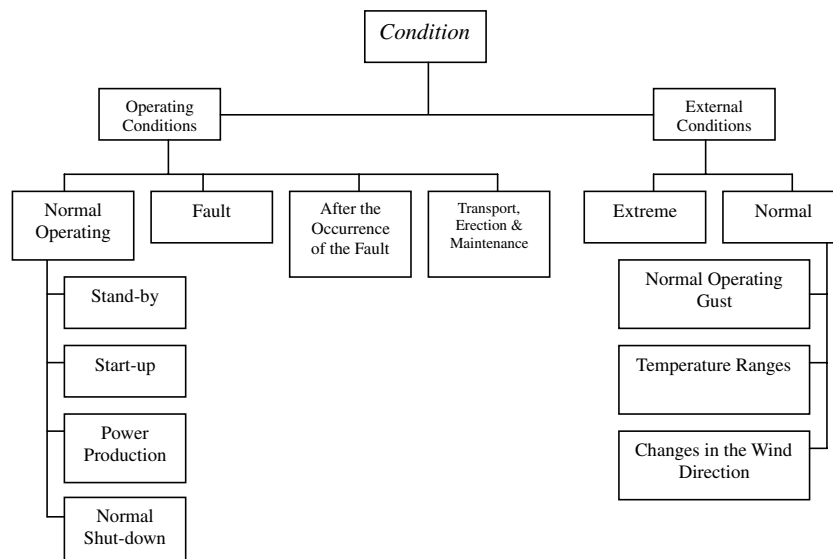


Fig. 6. General view of operating and external conditions of a wind turbine.

Table 7  
Static analysis of blade under different events

Events	Tip deflection [m]	Maximum longitudinal stress [MPa] (safety factor)	Maximum transverse stress [MPa] (safety factor)	Maximum in-plane shear stress [MPa] (safety factor)
Standby	1.23	520.12 (2.22)	13.61 (3.1)	21.33 (3.8)
Start-up	1.67	650.30 (1.79)	12.94 (2.8)	32.50 (2.5)
Power production	4.21	725.00 (1.60)	15.50 (2.3)	18.12 (4.4)
Shut-down	4.33	764.00 (1.52)	19.02 (1.9)	21.27 (3.8)

The safety factor results show that in all cases the structure is in a safe condition. Knowing that the tip-to-tower distance of the blade is 4.5 m, then for the maximum tip deflection case, tip of the blade will not hit the tower.

In the third step, the structure is studied under thermal loads and the analysis shows that the temperature range does not have a significant effect in comparison with other load cases, so the temperature load was not considered further.

In the fourth step, buckling phenomena was considered linearly and non-linearly and obtained results [12] indicate that the structure is in a safe condition.

The Tsai–Wu criterion is used to obtain the critical zone for failure. Furthermore, because of the existence of a pitch control system on the investigated blade and a rotation of the blade along its length by wind speed variation around 89°, the obtained critical zone by the Tsai–Wu criteria varied with the change in wind speed. The results showed that the critical zone can be divided into five groups for 4–8, 8–12, 12–16, 16–20 and 20–25 m/s wind speed ranges. From these ranges, the most probable wind speed range that has the biggest value as its accumulate wind speed probability is selected as the most critical zone. This zone is located on the upper flange of the spars, which has a layup with 11 layers of 0° and one [+45/–45]<sub>T</sub> bi-axial laminate.

Finally, a comparison between normalized longitudinal ( $N_X$ ), transverse ( $N_Y$ ) and shear forces ( $N_{XY}$ ) to the length of selected critical zone, proves that the quantity of  $N_Y$  and  $N_{XY}$  versus  $N_X$  is negligible and also, considering normalized moments ( $M_X$ ,  $M_Y$  and  $M_{XY}$ ) will not change the amount of effective stresses significantly. So it can be concluded that the uni-axial fatigue mode is dominant for the critical region.

## 7. Accumulated fatigue damage modeling

One of the presented techniques to investigate fatigue in composites is called “*Generalized Material Property Degradation Technique*” which was developed by Shokrieh and Lessard [13]. In this research, Shokrieh–Lessard’s method was simplified in order to simulate the laminated composite behavior under uni-axial fatigue loading. This model can estimate damage status at any stress level and number of cycles from start of loading

to sudden failure of the component and can predict final fatigue life. In order to fulfill the mentioned requirements, an accumulated fatigue damage model is suggested based on CLT<sup>1</sup> [14]. This model contains three main parts: stress analysis, damage estimation and material properties degradation. Due to this fact that the selected critical zone is placed in a confined region, edge effects will not occur and therefore CLT is appropriate. The flowchart of the accumulated fatigue damage that has been used for developing a computer code in order to calculate needed parameters is shown in Fig. 7.

As shown in Fig. 7, a proper model for stress analysis must first be developed. In this step, material properties, maximum and minimum fatigue load, maximum number of cycles, incremental number of cycles are defined. Then stress analysis based on CLT theory and loading condition is preformed. In the next step, failure analysis is preformed. If there is a sudden mode of failure, then material properties of the failed plies are changed according to appropriate *sudden* material property degradation rules. The stiffness matrix of the finite element model is rebuilt and the stress and failure analysis are preformed again. In this step, if there is no sudden mode of failure, an incremental number of cycles is applied. If the number of cycles is greater than a preset total number of cycles, then the computer program stops. Otherwise, stiffness of all plies (of all elements) is changed according to gradual material property degradation rules. Then stress analysis is performed again and the above loop is repeated until catastrophic failure occurs, or the maximum number of cycles (pre-defined by the user) is reached. It is necessary to mention that in the material property degradation, different methods have been experienced by several authors for strength degradation or stiffness degradation as a single criteria or combinations of stiffness and strength degradation as a combined criterion. In this study, in order to decrease run-time of model, the stiffness degradation technique was employed. In this method remaining stiffness of an U-D ply under desired uni-axial state of stress and desired stress ratio can be calculated using the following equation which is a modified and improved form of Ye’s model [15]:

<sup>1</sup> Classical lamination theory.

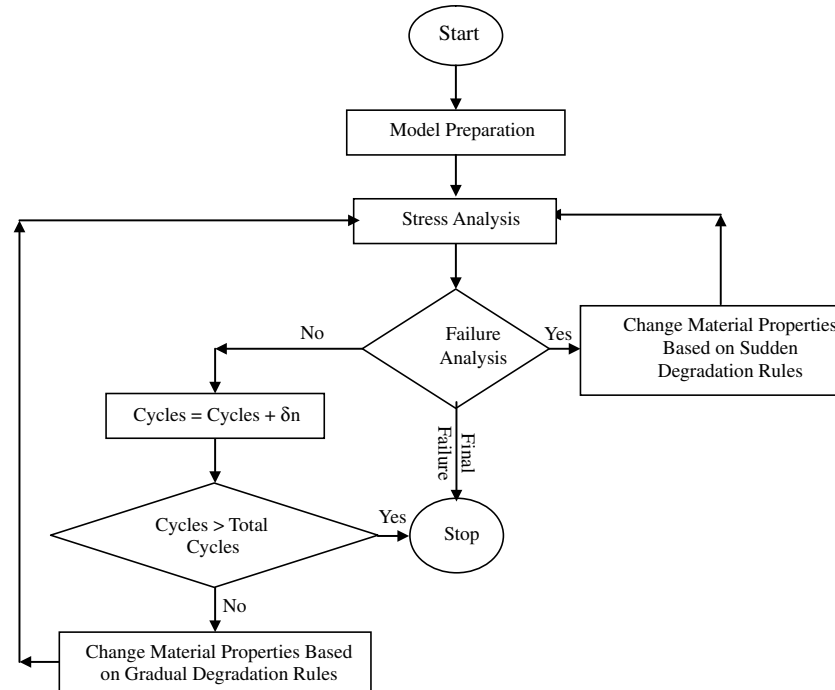


Fig. 7. Flowchart of accumulated fatigue damage modeling.

$$E(n, \sigma, \kappa) = \left(1 - \frac{\tilde{D}}{f(\sigma, \sigma_{ult})}\right) E_0$$

In this equation,  $E_0$ ,  $E(n, \sigma, \kappa)$  and  $\tilde{D}$ , respectively, represent initial stiffness before start of fatigue loading, residual stiffness (as a function of number of cycles, applied stress and stress ratio) and normalized damage parameter. Due to the fact that the amount of  $\tilde{D}$  does not depend on the applied stress level, in order to include the role of stress in the amount of damage  $f(\sigma, \sigma_{ult})$  is used. A complete form of  $f(\sigma, \sigma_{ult})$  was developed [13] based on available experimental data for carbon/epoxy (commercially called AS4/3501-6).

A developed damage estimation method is used to calculate  $\tilde{D}$  that describes a relation between  $\tilde{D}$  and  $\tilde{N}$ , which is called the normalized number of cycles. Available experimental data show that normalized damage increases linearly from start of loading till  $\tilde{N} = 0.67$  and after that the rate of damage increases non-linearly until final failure ( $\tilde{N} = 1$ ). So the relation between  $\tilde{D}$  and  $\tilde{N}$  can be divided into two phases. All equations that describe the linear and non-linear relations between  $\tilde{D}$  and  $\tilde{N}$  are fully constructed for both phases [16]. In all aforementioned equations,  $\tilde{N}$  is calculated using following equation:

$$\tilde{N} = \frac{\log(n) - \log(0.25)}{\log(N_f) - \log(0.25)}$$

where,  $n$  and  $N_f$  describe number of applied cycles and cycles to failure respectively.  $N_f$  must be calculated using following relation [13]:

$$\frac{\ln(a/f)}{\ln[(1-q)(C+q)]} = A + B \log N_f$$

where

$$q = \sigma_m / \sigma_r, \quad a = \sigma_a / \sigma_r, \quad C = \sigma_c / \sigma_r, \\ \sigma_m = \frac{(\sigma_{max} + \sigma_{min})}{2}, \quad \sigma_a = \frac{(\sigma_{max} - \sigma_{min})}{2}$$

It is shown that in shear loading, the aforementioned equation can be modified to the following form [13]:

$$u = \log \left( \frac{\ln(a/f)}{\ln[(1-q)(C+q)]} \right) = A + B \log N_f$$

where  $u$  and  $f$  are curve fitting parameters which have been obtained for AS4/3501 material [13].

## 8. Evaluation of accumulated fatigue damage model

The computer code which has been written on the *Mathematica* platform [17], was tested for a 0-degree U-D ply of carbon/epoxy under tensile longitudinal fatigue loading, a 90-degree U-D ply of carbon/epoxy under tensile transverse fatigue loading and a cross-ply of carbon/epoxy. The obtained results in comparison with available experimental data [13,18,19] are shown in Figs. 8–10 which explain the appropriate performance of model.

All equations and relations have been developed based on available experimental data for carbon/epoxy composites. Since normalized life curves for glass/epoxy

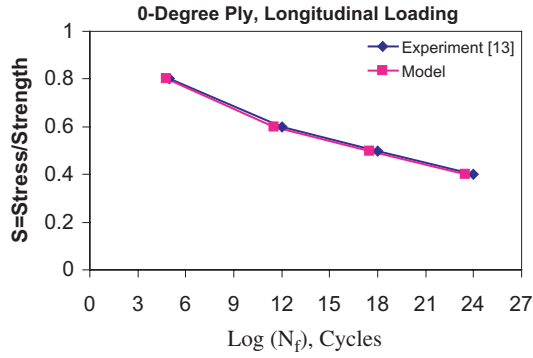


Fig. 8. Experimental data and results of computer code for 0-degree ply.

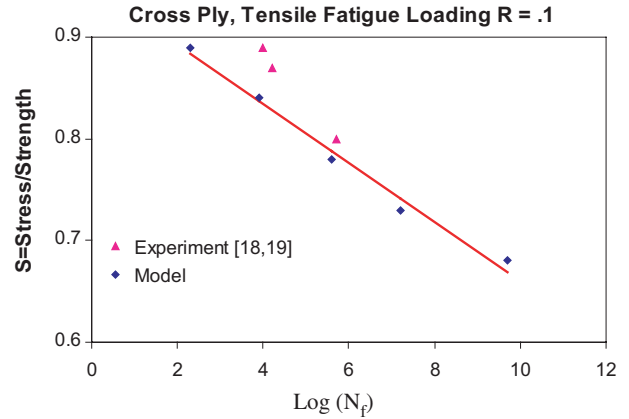


Fig. 10. Experimental data and results of computer code for cross ply.

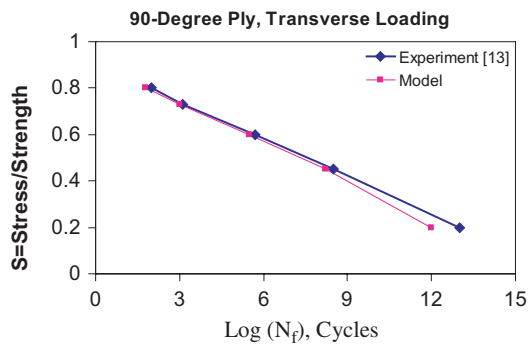


Fig. 9. Experimental data and results of computer code for 90-degree ply.

were not available, a generic behavior was estimated based on the pattern of decreasing mechanical properties and strengths of carbon/epoxy. The only available criteria for evaluation of aforementioned generic fatigue behavior process, is the mentioned criteria in MSU/DOE fatigue database [4] for wind turbine blade application. In MSU/DOE, the behavior of involved composite materials in blade structures is defined by the following equation [4]:

$$\sigma/\sigma_0 = 1 - b \log(N)$$

where “ $\sigma$ ” is maximum applied stress and “ $\sigma_0$ ” is corresponding static strength in the same direction of applied stress and finally “ $b$ ” is a parameter which varies for the

different materials. In MSU/DOE two magnitudes of “ $b$ ” were presented which describe two boundaries of all curves. The upper bound refers to good material that behaves perfectly against fatigue and the lower bound refers to poor material that behaves weakly. The values of “ $b$ ” for different fatigue loading situations are extracted from the MSU/DOE database [4] and inserted in Table 8.

After using the accumulated fatigue damage model, with aforementioned generic methods, the obtained results approach the bound of good materials as expected. For instance, tensile mode results are shown in Fig. 11. Good materials are those with high quality and same volume of resin at all points containing non-woven fabrics [4]. Since the pre-preg materials are known as materials that fulfill the above-mentioned characteristics, it can be concluded that the obtained results are logical and generic behavior is appropriate. However, it is necessary to mention that, even though the generic method is working properly, a more complete treatment would involve extracting the normalized life curve and other required parameters specifically for the type of glass/epoxy used here.

One of the most important advantages of using accumulated fatigue damage modeling is in its independence of lay-up configuration. Thus it can be used for any configuration of fabrics, knowing behavior of involved U-D

Table 8  
Values of “ $b$ ” for two bounds of good and poor materials ( $S-N$  data)

Type of data	Extremes of normalized $S-N$ fatigue data for fiberglass laminates		
Tensile fatigue data ( $R = \sigma_{\min}/\sigma_{\max} = 0.1$ )	Good materials $b = 0.1$	Poor materials $b = 0.14$	Normalization UTS <sup>a</sup>
Compressive fatigue data ( $R = 10$ )	Good materials $b = 0.07$	Poor materials $b = 0.11$	Normalization UCS <sup>b</sup>
Reversal fatigue data ( $R = -1$ )	Good materials $b = 0.12$	Poor materials $b = 0.18$	Normalization UTS

<sup>a</sup> Ultimate tensile strength.

<sup>b</sup> Ultimate compressive strength.

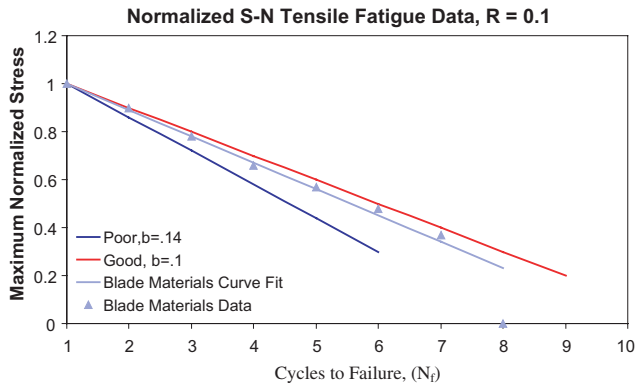


Fig. 11. Results of computer code based on used generic method in comparison with good and poor material data from MSU/DOE database.

plies (full characterization of each configuration is not required).

**9. Wind resource characterization**

Identification of governing wind patterns on the wind farm vicinity is necessary for weighting different events for fatigue analysis. The wind speed is never steady at any site, but it is rather influenced by the weather system, the local land terrain and the height above the ground surface. Therefore, annual mean speed needs to be averaged over 10 or more years. Such a long term average raises the confidence in wind speed distribution. However, long-term measurements are expensive, and most projects cannot wait that long. In such situations, the short term, say one year, data is compared with a nearby site having available long-term data to predict the long-term annual wind speed at the site under consideration. This is known as the “measure, correlate and predict (MCP)” technique. Since wind is driven by the sun and the seasons, the wind pattern generally repeats itself over the period of one year. The wind site is usually described by the speed data averaged over the calendar year. The wind speed variations over the period can be described by a probability distribution

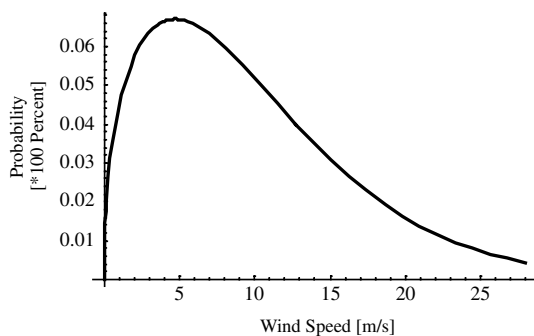


Fig. 12. Weibull distribution function of Manjil.

function in the form of a Weibull function. For this purpose the Weibull function of Manjil (a city in the north of Iran) was derived using metrological data in the following form [20]:

$$h(v) = \left(\frac{1.425}{9.3206}\right) \left(\frac{v}{9.3206}\right)^{(0.425)} e^{-\left(\frac{v}{9.3206}\right)^{1.425}}$$

where  $v$  is a wind speed and  $h(v)$  is the corresponding probability of occurrence. Fig. 12 shows this distribution.

**10. Fatigue investigation of the blade**

The main sources that produce cyclic loads on a wind turbine blade are the variation of wind speed, annual gust, rotation of rotor and variation of weight vector direction toward the local position of the blade [20]. The two first sources change the total amount of the load and the last one produces fluctuating load with a frequency identical to the rotor rotation frequency. Another source which produces cyclic loading on the blade is the effect of wind shear. This effect arises from change of wind speed by change in height. In the usual calculation, wind speed is measured at hub center of rotor and the effect of wind shear is not considered. It has been proven that the wind shear effect acts in-phase with the weight vector. It has been also shown that considering wind shear effect does not have any significant effect on fatigue damage [21], so this effect is not considered further in the design process. Gust occurrence is considered based on annual gust according to the Germnaschier Lloyds standard [11]. During gust occurrence, the blade is excited and vibrated by the linear combination of its mode shapes because of the gust impact effect. Eggleston and Stoddard suggest [22] that the higher order frequencies (>2 Hz) contribute around 15% to the overall displacements. Therefore, considering first mode shape excitation will be conservative enough. Considering the active yaw control system acting on the turbine, the change in wind direction effect is also negligible. Because the turbine always stays up-wind and whenever wind direction changes, the active yaw control system will adapt the turbine with new direction of wind vector in a very short period of time.

So, after defining cyclic loading sources, all corresponding applied stresses are derived from full range static analyses covering all events [20].

**11. STOFAT<sup>2</sup> computer code**

Since wind flow is random in its nature, considering deterministic fatigue analysis is not an appropriate ap-

<sup>2</sup> STOchastic FATigue.

proach. Traditionally, deterministic analysis was employed in fatigue calculation of a wind turbine blade and the effect of randomness was just considered by employing safety factors. Implementation of stochastic loading was considered using the Monte-Carlo simulation technique [23] so a computer code was established in this research. This computer program was named STOFAT. At first STOFAT produces a 30-year wind pattern in accordance with the extracted Weibull distribution in the earlier section. This pattern will satisfy randomness of both wind speed and its duration, as the two major sources of randomness. Namely, after generation of each wind speed, its duration will be randomly selected between zero and total predefined portion from Weibull probability distribution function. This process continuously generates wind speed and its portion until the accumulated portion of each wind speed reaches to its predefined amount. This code is also capable of considering an annual gust in wind pattern randomly in both wind speed and its position in the wind pattern. The duration of gust is considered to be one hour as dictated by rules of the standard [11]. After generation of wind patterns for 30 years, in each event, STOFAT calls the “accumulated fatigue damage model” as a subroutine in order to perform fatigue calculations. The run-time of STOFAT is 2.5 h in a computer with 2.4 GHz processor which is powered by 512 MB of RAM memory.

**12. Results**

In order to perform fatigue analysis, the computer code was executed 50 times. The estimated blade lifetime is shown in Fig. 13. One can observe that the results are bounded by 24 and 18.66 years as the upper and lower limits, while the average is 21.33 years. The corresponding standard deviation of the obtained results is equal to 1.59 years. Since wind patterns in the investigated region (Manjil) and consequently the applied load on a blade is never deterministic, proper scatter in the obtained results implies a proper fatigue modeling.

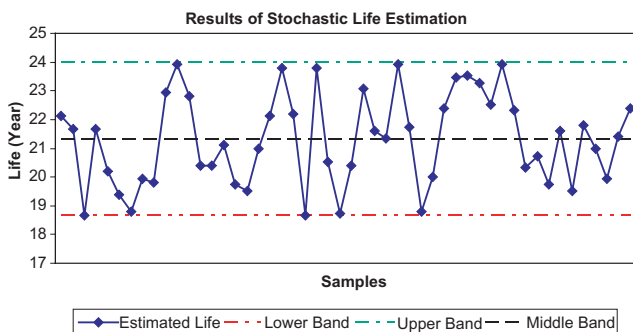


Fig. 13. Predicted lifetime of blade by STOFAT computer code and for 50 runs.

Table 9  
Fatigue failure trend for one obtained result from STOFAT computer code

Layer no.	Lay-up	Year of failure
1	+45	9.3
2	-45	10.6
3	0	13.13
4	0	15.6
5	0	16.3
6	0	17.2
7	0	18.06
8	0	18.66
9	0	18.73
10	0	18.8
11	0	19
12	0	19.2
13	0	19.3

One of the obtained results was randomly selected and the progress of fatigue failure was followed step-by-step to assure performance of code. This is shown in Table 9.

The results prove that damage progress is logical and the code can model it properly.

**13. Conclusion**

In this study, the accumulated fatigue damage model was presented and applied based on CLT. that employs stiffness degradation as a single measure of damage estimation. Several checks were carried out on the model in order to assure proper simulation of the damage progress. All load cases are identified, calculated and evaluated and negligible cases are ignored. By performing finite element modeling, the critical zone of the blade is obtained. Fatigue phenomenon is studied in the selected critical zone using accumulated fatigue damage modeling. Based on a stochastic approach, random load cases are weighted by their rate-of-occurrence from wind patterns of the Manjil region. The results are bounded between 18.66 years and 24 years as lower and upper limits. Moreover, 1.59 years as the standard deviation shows a small range of scatter in the range of obtained results. These results show that presented accumulated fatigue damage model and the employed stochastic method are able to simulate the fatigue damage progress in a wind turbine composite blade. Considering the conservative nature of the employed technique, the investigated blade will have 18.66 years in the worse situation and 24 years in the best situation.

**References**

[1] Spera DA, editor Wind turbine technology. New York: ASME Press; 1994.

- [2] Sutherland HJ. On the fatigue analysis of wind turbines. Sandia National Laboratories, Albuquerque, New Mexico, June 1999, SAND99-0089.
- [3] Mandel JF, Samborsky DD, Cairns DS. Fatigue of composite materials and substructures for wind turbine blades. Sandia National Laboratories, Albuquerque, New Mexico, March 2002, SAND2002-0771.
- [4] DOE/MSU Composite Materials Fatigue Database, February 26, 2003. Sandia National Laboratories, Albuquerque, New Mexico.
- [5] Auto-CAD user manual, Release 2002.
- [6] ANSYS Ver. 5.4 User Manual, SAS Co, 1998.
- [7] Tsai SW, Hoa SV, Gay D. Composite materials, design and applications. CRC Press; 2003.
- [8] HexPly Data Sheets, M9.6 Series for Wind Turbine Blade Application, Hexcel Composites Co., France Branch, 2002.
- [9] Shokrieh MM, Rafiee R. Extraction of required mechanical properties for FEM analysis of multidirection composites using CLT approach. CANCOM, 2005, Vancouver, Canada, accepted.
- [10] Tsai SW, Thomas Hahn H. Introduction to composite materials. USA: Technomic Publishing Co; 1980.
- [11] Lloyd G. Rules and regulations. Non-marine technology, Part IV, Regulation for the certification of wind energy conversion system. Definition of load cases, Chapter 4, 1993.
- [12] Shokrieh MM, Rafiee R. Stochastic analysis of fatigue phenomenon in a HAWT composite blade. Sharjah: ICCST; 2004. p. 197–202.
- [13] Shokrieh M, Lessard LB. Progressive fatigue damage modeling of composite materials, Part I: Modeling. *J Compos Mater*, USA 2000;34(13):1056–80.
- [14] Hull D. An Introduction to Composite Materials. Press Syndicate of the University of Cambridge; 1981.
- [15] Ye, Lin. On fatigue damage accumulation and material degradation in composite materials. *Compos Sci Technol* 1989;36:339–50.
- [16] Shokrieh MM, Zakeri M. Evaluation of fatigue life of composite materials using progressive damage modeling and stiffness reduction. In: Proceedings of the 11th annual conference of mechanical engineering, Iran, Mashhad, 2003. p. 1256–63.
- [17] The Mathematica Book, STEPHEN WOLFRAM, 4th ed., Mathematica Version 4, 1999.
- [18] Charewics A, Daneil IM. Damage mechanics and accumulation in graphite/epoxy laminates. In: Hahn HT, editor. *Composite materials: fatigue and fracture*. ASTM STP 907, 1986. p. 247–97.
- [19] Lee JW, Daniel IM, Yaniv G. Fatigue life prediction of cross-ply composite laminated. In: Lagace PA, editor. *Composite materials: fatigue and fracture*. ASTM STP 1012, vol. 2, 1989. p. 19–28.
- [20] Shokrieh MM, Rafiee R. Lifetime prediction of HAWT composite blade. In: 8th international conference of mechanical engineering, Tehran, 2004. p. 240.
- [21] Noda M, Flay RGJ. A simulation model for wind turbine blade fatigue loads. *J Wind Eng Ind Aerodynam* 1999;83:527–40.
- [22] Eggleston DM, Stoddard FS. *Wind turbine engineering design*. New York: Van Nostrand Reinhold; 1978.
- [23] Kleiber M, Hien TD. *The stochastic finite element method*. New York: John Wiley Publisher Science; 1992.